Electronic supplementary information (ESI)

Huaizhi Yang, ‡ [a] Yuqi Wan, [a,b] Qingrong Cheng, *[a] Hong Zhou, [a] Zhiquan Pan[a]

[a] School of Chemistry and Environmental Engineering, Wuhan Institute of Technology, Wuhan, 430205, PR China.

[b] Department of Chemistry, City University of Hong Kong, Hong Kong, 99907, PR China

Corresponding authors:

*(Q.C.) E-mail: chengqr383121@sina.com

‡These authors contributed equally to this work.

Total number of pages: 10

Total number of Tables: 3

Total number of Figures: 7

Characterization methods

A scanning electron microscope (SEM, Zeiss Gemini 300) was used to observe the external morphology of all samples, and the basic element composition distribution (EDS) was obtained by equipped with an energy dispersive X-ray spectrometer. Transmission electron microscopy (TEM, TitanG2 60-300) was used to characterize the internal and microstructural information of the samples (HRTEM measures the lattice information of substances). Fourier Transform Infrared Spectroscopy (FT-IR) was acquired on a Nicolet 6700 spectrophotometer to analyze characteristic functional group changes in the wavelength range of 4000–400 cm^{-1} (KBr pellets). Ultraviolet-Visible (UV-Vis) diffuse reflectance spectroscopy (DRS) was measured using a West Wisteria UV-2600 spectrometer with barium sulfate as a reference. Mott-Schottky's measurement experiments were performed on a CHI 660E electrochemical system (Chenhua, Shanghai, China) at frequencies from 1000 Hz to 500 Hz, and the potential changes from -2.0 to 1.5 eV concerning Ag/AgCl. X-ray photoelectron spectroscopy (XPS) was performed using the 250Xi-XPS photoelectron spectrometer of the thermal calibration laboratory and aluminum Kα ray resources. The change in binding energy was taken as the internal standard at the c1s level at 284.6 eV. The patterns collected on a BrukerD8 advanced X-ray diffractometer (XRD) were used to analyze the surface phase composition of the materials, scans over a test angle range of 0.5° to 5° at a rate of 1° min^{-1}, and scans over a test angle range of 5° to 90° at a rate of 5° min^{-1}. Measurements of specific surface area and pore structure were performed using Brunauer-Emmett-Teller (BET, Micro), ESR measured by German Bruker (A300), it is used to detect the content of $\bullet O_2^-$ and •OH in the process of photoreaction.

Electrochemical measurements were carried out on an electrochemical workstation (Zahner, Zennium) connected to a standard three-electrode system, namely the working electrode prepared from the test sample, a platinum plate as the counter electrode, and a saturated Ag/AgCl as the reference electrode. The working electrode was prepared as follows: Weigh 10mg of the sample and pour it into a 5 mL EP tube, add 2 mL Nafion injection solution (Nafion: isopropanol = 1:25), and sonicate for 15 min. Each time, 10 microliters were dropped onto the conductive glass surface with a micro-injector, dispersed evenly, and dried under a sun lamp, and the operation was repeated 3 times. The test solution for both is a 0.5 M sodium sulfate aqueous solution, which is required to submerge the three electrodes. Electrochemical impedance spectroscopy (EIS) data were measured

directly at the electrochemical workstation, the frequency range of the circuit potential was 0.1 Hz to 100 kHz, and the test voltage was 1.5 eV. Transient Photocurrent Response (PC) of the sample was carried out under visible light conditions (300 W xenon lamp, with 420 nm filter), with the light on for 30 s and the light off for 30 s as a cycle, for 5 consecutive cycles.

Evaluation of Photocatalytic Performance

Photocatalysis experiments include organic pollutant degradation experiments and hydrogen production experiments. The ability of photocatalysts to degrade organic pollutants can be judged by measuring the changes in the absorbance (positions of characteristic peaks) of organics under visible light irradiation. The light source is visible light (with a 420 nm filter). First, 50 mL of 40 mg/L TC solution was poured, 3 mL of the solution was taken out, and the measured absorbance was recorded as the initial absorbance (C_{-30}). Then, 10mg of the photocatalyst was added, and the catalyst was magnetically stirred for 30 min in the dark to reach the adsorption-desorption equilibrium. After the light-proof treatment, 3 ml of the solution was taken out, and the measured absorbance was recorded as the absorbance at 0 min of illumination (C_0). During the photoreaction, 3 mL samples were withdrawn from the reactor every 10 min (It is represented by C_t, and it is denoted as C_{10} and C_{20} in turn.). All samples were filtered photocatalysts using organic filters (0.22 μm. organic). The absorption intensity at the maximum wavelength of 357 nm was measured with a UV-Vis spectrophotometer, and the concentration change was reflected by the change of absorbance to evaluate the degradation efficiency.

In the photocatalytic degradation cycle experiments, the products were collected by a common centrifugation method. Considering the mass loss, the amount of catalyst added was changed to 20 mg. In each cycle, we only collected samples before dark (C_{-30}), after dark (C_0), and after 60 min of light (C_{60}). At the end of a cycle, the catalyst in the remaining liquid was collected by centrifugation and washed with methanol and after vacuum drying, and then enter a new round of photocatalytic degradation test with a new tetracycline solution. A total of four cycles were carried out to test the stability of the prepared composite photocatalyst.

The photocatalytic hydrogen production experiments were carried out in a 150 mL cylindrical quartz reactor with an irradiation area of 28.12 cm^2 and a 300 W xenon lamp (with a 420 nm filter) as the

light source (PerfectLight, Labsolar-IIIAG Photocatalytic system). Mixed 30 mg of photocatalyst, 80 mL of distilled water, and the prepared sacrificial agent (10 mL of 0.35 M sodium sulfite solution, 10 mL of 0.25 M sodium sulfide solution) evenly, and replace the air in the container with nitrogen before the reaction, turn on stirring and keep the catalyst suspended in the reaction system, use a syringe needle draws 300 μL of gas per hour from the reactor, and the H_2 generation rate is calculated by gas chromatography (Timei GC7900, TCD, N_2 as carrier). The operation of the photocatalyst cycle test is as follows: after the first hydrogen production experiment under visible light, the photocatalyst is collected by centrifugation, washed three times with ethanol, the obtained solid is dried, and transferred to a new solution system, filled with nitrogen again, and carried out for the next hydrogen production experiment, the entire process was repeated four times.

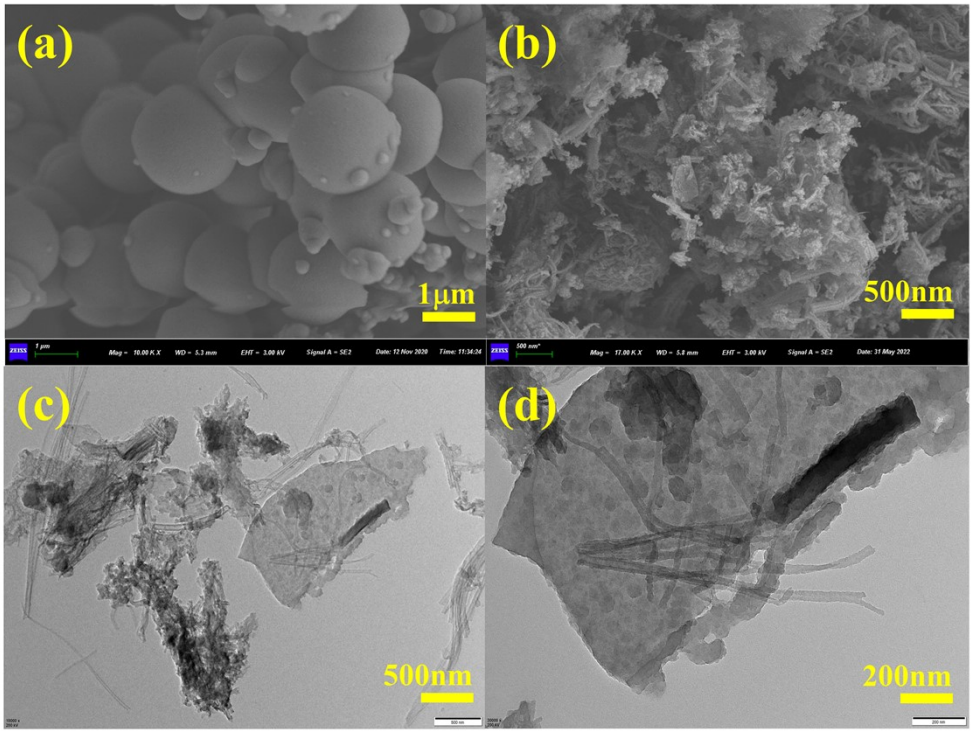

Fig.S1 (a) SEM image of LZU-1 (b) SEM image of HLZU-1 (c, d) TEM image of HLZU-1 in size of 200 nm and 500 nm, respectively.

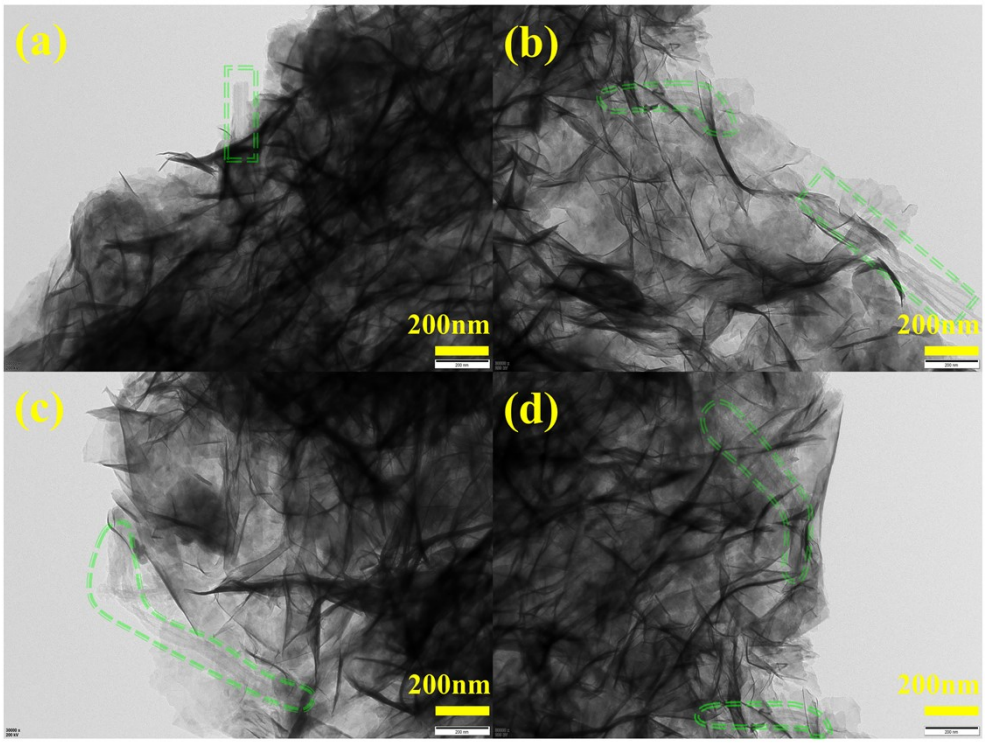

Fig.S2 (a-d) The magnified TEM images of the upper left, upper right, lower left and lower right corners of Fig. 2(b), respectively.

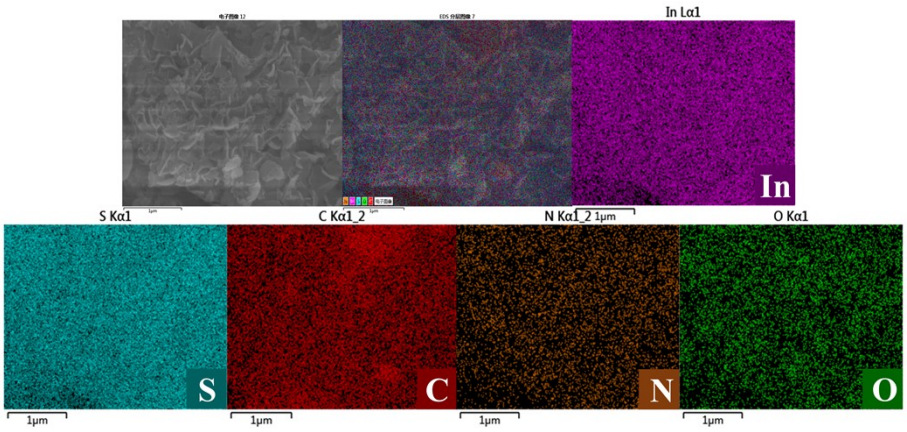

Fig.S3 In, S, C, N, and O EDX mapping of the composite IL-1.

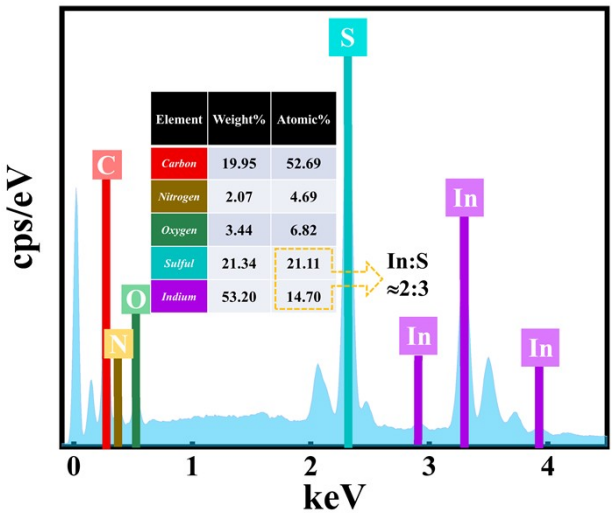

Fig.S4 EDS plot of the composite material. Illustration: A table showing the content of different elements.

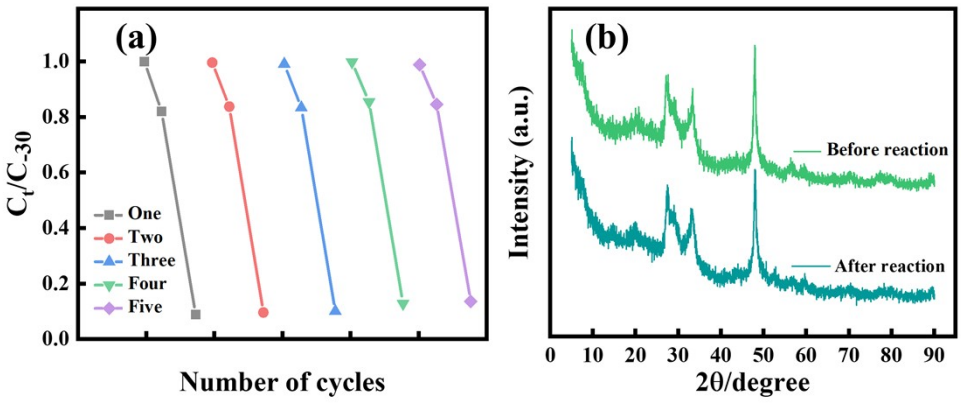

Fig.S5 (a) Photocatalytic effect of IL-1 in five cycles. (b) XRD patterns of IL-1 before and after cycling.

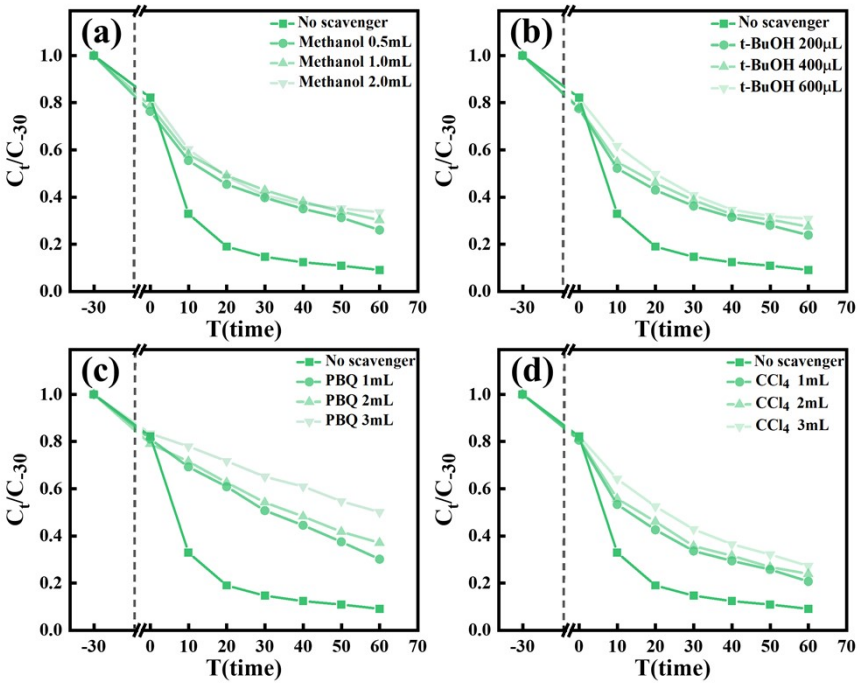

Fig.S6 (a-d) The radical trapping test for the IL-1.

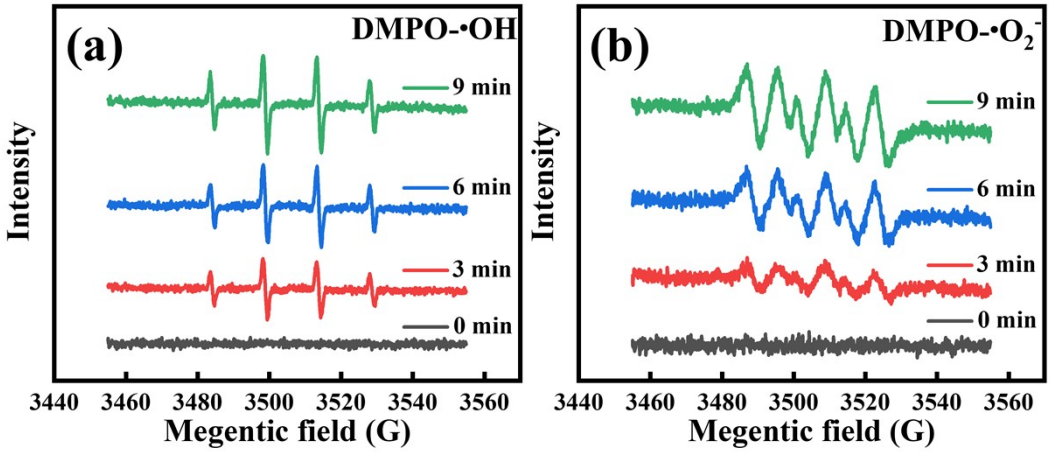

Fig.S7 The ESR spectrum of IL-1 for DMPO–•OH and DMPO–•O_2^-.

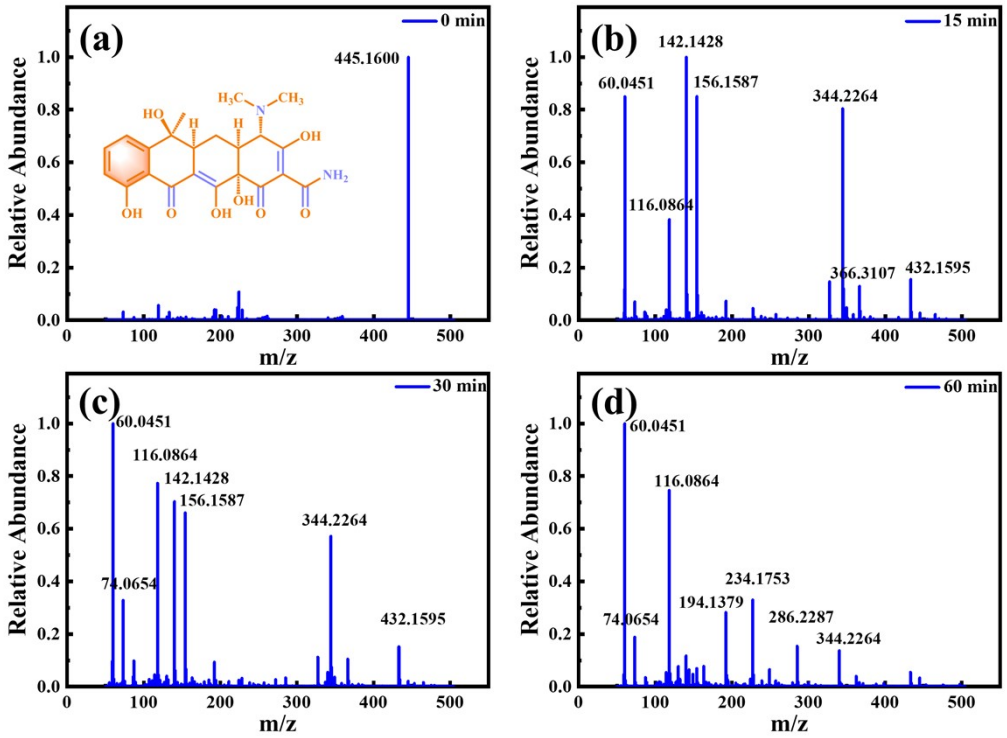

Fig.S8 (a-d) are the LC-MS spectra of 0 min, 15 min, 30 min and 60 min of light during TC degradation, respectively.

Table S1 The dosage of various raw materials in the synthesis of composite materials (IL-x(x=1-3)).

Catalyst name	*HLZU-1/mg*	*$In(NO_3)_3{\cdot}xH_2O$/mg*	*H_2BDC/mg*	*DMF/mL*
IL-1	20	160	80	18
IL-2	35	130	65	16
IL-3	60	120	60	16

Table S2 Comparison of TC degradation over IL-1 and other photocatalysts.

Catalyst / mg	*V (mL) / C_{-30} ($mg{\cdot}L^{-1}$)*	*Light source*	*Time (min)*	*Result (%)*	*TOF*	*Ref*
In_2S_3/HLZU-1/10	50/30	Visible light	60	90.1%	2.275	This work

In_2S_3/MIL-100(Fe)/30	100/10	Visible light	90	88%	0.326	1
In_2S_3/$InVO_4$ /50	100/10	Visible light	60	71.4%	0.238	2
In_2S_3 /$Bi_2O_2CO_3$/30	30/10	Visible light	180	70%	0.039	3
MWCNT@MOF-derived In_2S_3/15	50/30	Visible light	120	100%	0.833	4
In_2S_3@MIL-125(Ti)/30	46/100	Visible light	60	63.3%	1.618	5

TOF is calculated according to an equation:

$$TOF = \frac{C_{-30} \times V_{TC} \times \text{Degradation rate}}{m_{\text{catalyst}} \times t}$$

Table S3 Comparison of the photocatalytic H_2 evolution rates over different photocatalysts.

Photocatalysts	***Irrigation***	***Sacrificial agents***	***Activity μmol·g^{-1}h^{-1}***	***Ref***
IL-1	Visible light	Na_2SO_3 and Na_2S	11920.42	This work
GO/Fe_2P/In_2S_3	Visible light	Ascorbic acid	483.22	6
In_2S_3/ TiO_2	Visible light	Methanol	637.9	7
Mo_2C- In_2S_3	Visible light	Lactic acid	535.58	8
In_2O_3/O_V/ In_2S_3	Visible light	Na_2S and Na_2SO_3	19	9
3wt%TiN−0.3wt%Pt@ In_2S_3	Visible light	Lactic acid	4397.5	10
LZU1@WO_3	Visible light	Na_2SO_3 and Na_2S	6133.2	11

References

1. Y. He, W. Dong, X. Li, D. Wang, Q. Yang, P. Deng and J. Huang, Modified MIL-100(Fe) for enhanced photocatalytic degradation of tetracycline under visible-light irradiation, J Colloid Interface Sci, 2020, 574, 364-376.
2. X. Yuan, L. Jiang, J. Liang, Y. Pan, J. Zhang, H. Wang, L. Leng, Z. Wu, R. Guan and G. Zeng, In-situ synthesis of 3D microsphere-like $In_2S_3/InVO_4$ heterojunction with efficient photocatalytic activity for tetracycline degradation under visible light irradiation, Chem. Eng. J, 2019, 356, 371-381.
3. H. Fan, H. Zhou, W. Li, S. Gu and G. Zhou, Facile fabrication of 2D/2D step-scheme $In_2S_3/Bi_2O_2CO_3$ heterojunction towards enhanced photocatalytic activity, Appl. Surf. Sci., 2020, 504, 144351.
4. Y. Pi, S. Jin, X. Li, S. Tu, Z. Li and J. Xiao, Encapsulated MWCNT@MOF-derived In_2S_3 tubular heterostructures for boosted visible-light-driven degradation of tetracycline, Appl. Catal., B, 2019, 256, 117882.
5. H. Wang, X. Yuan, Y. Wu, G. Zeng, H. Dong, X. Chen, L. Leng, Z. Wu and L. Peng, In situ synthesis of In_2S_3@MIL-125(Ti) core–shell microparticle for the removal of tetracycline from wastewater by integrated adsorption and visible-light-driven photocatalysis, Appl. Catal., B, 2016, 186, 19-29.
6. X. Li, X. Lyu, X. Zhao, Y. Zhang, S. N. Akanyange, J. C. Crittenden, H. Zhao and T. Jiang, Enhanced photocatalytic H_2 evolution over In_2S_3 via decoration with GO and Fe_2P co-catalysts, Int. J. Hydrogen Energy, 2021, 46, 18376-18390.
7. Q. Hu, G. Chen, Y. Wang, J. Jin, M. Hao, J. Li, X. Huang and J. Jiang, Enhancing photocatalytic H_2 evolution on In_2S_3/mesoporous TiO_2 nanocomposites via one-pot microwave-assisted synthesis using an ionic liquid, Nanoscale, 2020, 12, 12336-12345.
8. X. Ma, C. Ren, H. Li, X. Liu, X. Li, K. Han, W. Li, Y. Zhan, A. Khan, Z. Chang, C. Sun and H. Zhou, A novel noble-metal-free Mo_2C-In_2S_3 heterojunction photocatalyst with efficient charge separation for enhanced photocatalytic H_2 evolution under visible light, J Colloid Interface Sci, 2021, 582, 488-495.
9. L. Wang, L. Zhang, H. Zhang, N. Li, S. Zhu, W. Li, W. Ran, Z. Jing and T. Yan, Construction of Dual‐tight Contact Interface in Z‐scheme System of In_2O_3/OV/In_2S_3 for Enhancing Photocatalytic Performance, ChemCatChem, 2021, 13, 2379-2385.
10. S. Liu, W. Qi, S. Adimi, H. Guo, B. Weng, J. P. Attfield and M. Yang, Titanium Nitride-Supported Platinum with Metal-Support Interaction for Boosting Photocatalytic H_2 Evolution of Indium Sulfide, ACS Appl Mater Interfaces, 2021, 13, 7238-7247.
11. S. Shang, H. Yang, D. Shi, B. Dong, H. Zhang, Q. Cheng and Z. Pan, Construction of LZU1@WO_3 heterojunction photocatalysts: enhanced photocatalytic performance and mechanism insight, New J. Chem., 2021, 45, 17025-17036.